

# TRPA1 mediates formalin-induced pain

Colleen R. McNamara\*, Josh Mandel-Brehm\*, Diana M. Bautista<sup>†</sup>, Jan Siemens<sup>†</sup>, Kari L. Deranian\*, Michael Zhao\*, Neil J. Hayward\*, Jayhong A. Chong\*, David Julius<sup>†\*</sup>, Magdalene M. Moran<sup>\*\*</sup>, and Christopher M. Fanger\*

\*Hydra Biosciences, Inc., 790 Memorial Drive, Cambridge, MA 02139; and <sup>†</sup>Departments of Physiology and Cellular and Molecular Pharmacology, University of California, San Francisco, CA 94143

Contributed by David Julius, July 5, 2007 (sent for review June 18, 2007)

The formalin model is widely used for evaluating the effects of analgesic compounds in laboratory animals. Injection of formalin into the hind paw induces a biphasic pain response; the first phase is thought to result from direct activation of primary afferent sensory neurons, whereas the second phase has been proposed to reflect the combined effects of afferent input and central sensitization in the dorsal horn. Here we show that formalin excites sensory neurons by directly activating TRPA1, a cation channel that plays an important role in inflammatory pain. Formalin induced robust calcium influx in cells expressing cloned or native TRPA1 channels, and these responses were attenuated by a previously undescribed TRPA1-selective antagonist. Moreover, sensory neurons from TRPA1-deficient mice lacked formalin sensitivity. At the behavioral level, pharmacologic blockade or genetic ablation of TRPA1 produced marked attenuation of the characteristic flinching, licking, and lifting responses resulting from intraplantar injection of formalin. Our results show that TRPA1 is the principal site of formalin's pain-producing action *in vivo*, and that activation of this excitatory channel underlies the physiological and behavioral responses associated with this model of pain hypersensitivity.

analgesia | inflammation | trp channel | formaldehyde

The formalin model was developed >30 years ago to assess pain and evaluate analgesic drugs in laboratory animals (1). In this test, a dilute (0.5–5%) formalin solution (in which formaldehyde is the active ingredient) is injected into the paw of a rodent, and pain-related behaviors are assessed over two temporally distinct phases, including an initial robust phase in which paw lifting, licking, and flinching are scored during the first 10 min, followed by a transient decline in these behaviors and a subsequent second phase of behavior lasting 30–60 min (2, 3).

Compounds that typically affect the first phase (Phase I) include local anesthetics, such as lidocaine (4). The second phase (Phase II) is proposed to result from activity-dependent sensitization of CNS neurons within the dorsal horn (3, 5, 6). Many analgesics, including intrathecal nonsteroidal antiinflammatory drugs (7), NMDA antagonists (8, 9), morphine (1, 10), and gabapentin (11, 12), inhibit only Phase II responses, but not Phase I.

The formalin test has several advantages over other models, in that spontaneous pain-related responses can be observed in a freely moving unrestrained animal. Once injected, no additional stimulus is required to evoke nocifensive behaviors, and behaviors can be scored over a prolonged period such that the precise onset and duration of analgesics can be assessed (1). However, despite the utility and widespread use of the formalin model in pain research, the mechanism by which formalin triggers C-fiber activation remains unknown (13) and is often attributed to tissue injury (1, 3, 9).

In this study, we show that formalin activates primary afferent sensory neurons through a specific and direct action on TRPA1, a member of the Transient Receptor Potential family of cation channels that is highly expressed by a subset of C-fiber nociceptors (14–17). TRPA1 is activated by a number of irritants that

cause pain, including allyl isothiocyanate (AITC) (17) and allicin (18, 19), the pungent ingredients in mustard and garlic extracts, respectively; as well as  $\alpha,\beta$ -unsaturated aldehydes, such as acrolein, that mediate the irritant actions of air pollutants (20). Sensory neurons from TRPA1-deficient mice show greatly diminished responses to each of these compounds, demonstrating that the TRPA1 channel is the primary molecular site through which they activate the pain pathway (20, 21). Recent studies have shown these irritants activate TRPA1 through an unusual mechanism involving covalent modification of cysteine and lysine residues within the N-terminal cytoplasmic domain of the channel protein (22, 23). Formaldehyde resembles these compounds, particularly acrolein, in regard to structure and chemical reactivity [supporting information (SI) Fig. 6], and thus we assessed whether TRPA1 activation could account for the excitatory actions of formalin on primary afferent nociceptors.

Here, we demonstrate that formalin activates TRPA1 in a heterologous expression system as well as isolated sensory neurons from dorsal root ganglia (DRG) or trigeminal sensory ganglia. Moreover, blockade of TRPA1 *in vivo* using either a specific antagonist or through disruption of the TRPA1 gene substantially attenuates pain-related responses to formalin. These findings demonstrate that formalin elicits primary sensory neuron excitation and pain through direct activation of TRPA1.

## Results

**Formalin Activates TRPA1.** We generated HEK293 cell lines stably expressing either human (hTRPA1) or rat TRPA1 (rTRPA1) and assessed their sensitivity to chemical stimuli using live-cell calcium imaging. Consistent with previous observations (17, 20), AITC evoked a dose-dependent  $\text{Ca}^{2+}$  rise in hTRPA1- and rTRPA1-expressing cells ( $\text{EC}_{50}$  of  $1.9 \pm 0.1$  and  $5.2 \pm 0.2 \mu\text{M}$ , respectively; Fig. 1A) but not in untransfected HEK293 cells or in cells expressing other sensory TRP channels, including hTRPV1, hTRPV3, or hTRPV4 (SI Fig. 7). Formalin also elicited  $\text{Ca}^{2+}$  influx in TRPA1-transfected cells, but not in parental or other TRP channel-expressing lines (Fig. 1B). The maximal response evoked by formalin was similar to that evoked by AITC. The  $\text{EC}_{50}$  values for formalin-evoked activation of hTRPA1 or rTRPA1 were  $0.0016 \pm 0.0001\%$  and  $0.0015 \pm 0.0001\%$ , respectively ( $\approx 200 \mu\text{M}$ ; Fig. 1C). Methanol, which is

Author contributions: C.R.M. and J.M.-B. contributed equally to this work; C.R.M., J.M.-B., D.M.B., J.S., N.J.H., D.J., M.M.M., and C.M.F. designed research; C.R.M., J.M.-B., D.M.B., J.S., K.L.D., and M.Z. performed research; C.R.M., J.M.-B., D.M.B., J.S., M.Z., J.A.C., D.J., M.M.M., and C.M.F. analyzed data; and C.R.M., D.M.B., J.S., J.A.C., D.J., M.M.M., and C.M.F. wrote the paper.

Conflict of interest statement: This study was carried out in collaboration with scientists at Hydra Biosciences, Inc., a startup biotechnology company in Cambridge, MA. D.J. serves as a member of the Hydra Biosciences Scientific Advisory Board.

Freely available online through the PNAS open access option.

Abbreviations: AITC, allyl isothiocyanate; hTRPA1, human TRPA1; rTRPA1, rat TRPA1; DRG, dorsal root ganglion.

<sup>†</sup>To whom correspondence may be addressed. E-mail: julius@cmp.ucsf.edu or mmoran@hydrabiosciences.com.

This article contains supporting information online at [www.pnas.org/cgi/content/full/0705924104/DC1](http://www.pnas.org/cgi/content/full/0705924104/DC1).

© 2007 by The National Academy of Sciences of the USA

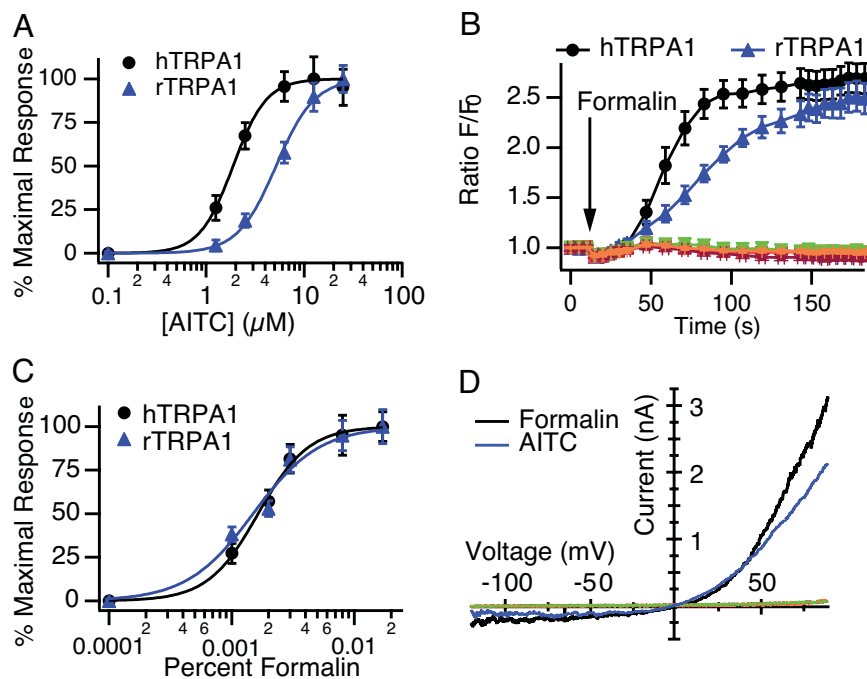


**Fig. 1.** TRPA1 is activated by formalin. Fluo-4  $\text{Ca}^{2+}$  responses of HEK-293 cells expressing human (black) or rat (blue) TRPA1. AITC- (A) or formalin- (C) induced concentration/response curves. Each point represents the average response of 49 experiments,  $\approx 3$  min after stimulation. (B) Representative experiment displaying full time course of the calcium response to formalin (0.01%). Parental cells (red) and cells expressing human TRPV1 (magenta), TRPV3 (orange), or TRPV4 (green) were unresponsive to formalin. (D) Representative current-voltage relationship of whole-cell currents evoked in TRPA1-expressing cells by formalin (0.01%; black) or AITC (5  $\mu\text{M}$ ; blue). Parental cells (red) and cells expressing human TRPV1 (magenta), TRPV3 (orange), or TRPV4 (green) were unresponsive. Currents were recorded in response to a 400-ms voltage ramp from  $-120$  to  $+100$  mV;  $n = 5$  per agonist.

used as a stabilizer in aqueous formalin solutions, did not evoke TRPA1 activation (data not shown), indicating that responses are caused by formaldehyde itself rather than vehicle components.

We next used whole-cell patch-clamp recording methods to directly assess formalin-evoked membrane currents in TRPA1-expressing HEK293 cells. Both AITC and formalin evoked outwardly rectifying currents that had a reversal potential near  $+5$  mV (Fig. 1D) and were attenuated by the nonselective TRP channel inhibitor, ruthenium red (14, 17, 24) (data not shown). Such currents were not induced by 0.15% methanol. Formalin activated hTRPA1 currents with an  $\text{EC}_{50}$  of  $0.003\% \pm 0.0002$  ( $\approx 400$   $\mu\text{M}$ ). The  $\text{EC}_{50}$  for AITC was consistent with previous reports, and current amplitudes elicited by AITC and formalin were comparable (Fig. 1D).

**Identification of a Specific TRPA1 Inhibitor.** Further characterization of the formalin-induced response was facilitated through the discovery of a potent and selective TRPA1 antagonist. To identify such a blocker, we screened a diverse small-molecule library for compounds that could inhibit the AITC-induced  $\text{Ca}^{2+}$  increase in TRPA1-expressing cells. One such compound (HC-030031; SI Fig. 6) was found to antagonize AITC- and formalin-evoked calcium influx with  $\text{IC}_{50}$  values of  $6.2 \pm 0.2$  and  $5.3 \pm 0.2$   $\mu\text{M}$ , respectively (Fig. 2A and B).

To confirm a direct action of HC-030031 on the TRPA1 current, we performed perforated-patch voltage-clamp recordings on TRPA1-expressing HEK293 cells. Both inward and outward currents elicited by AITC or formalin were rapidly and reversibly blocked by HC-030031 (Fig. 2C and D). We also found that HC-030031 blocked activation of TRPA1 by *N*-methyl maleimide, which opens the channel irreversibly through cysteine modification (22) (data not shown).  $\text{IC}_{50}$  values for TRPA1 blockade by HC-030031 or ruthenium red were similar to those

observed in the  $\text{Ca}^{2+}$  imaging experiments (Fig. 2). HC-030031 did not block currents mediated by TRPV1, TRPV3, TRPV4, hERG, or NaV1.2 channels (Table 1). Finally, we examined other mammalian TRPA1 orthologues (rat and mouse) and found that these channels resembled hTRPA1 in their sensitivity to activation by formalin and to block by HC-030031 (data not shown). Taken together, these results show that, at the doses tested, formalin specifically activates recombinant TRPA1 channels, and that HC-030031 is a potent and selective inhibitor of TRPA1 *in vitro*.

**Formalin Activates TRPA1 in Isolated DRG Neurons.** To identify the native target of formalin action, we used calcium imaging to ask whether formalin activates dissociated sensory neurons from rodent DRG and trigeminal ganglia. Approximately 30% of cultured neurons from WT mouse ganglia showed robust increases in intracellular free calcium after application of Ringer's solution containing 0.01% formalin (Fig. 3A). Subsequent application of AITC induced a slight increase in calcium in all formalin-sensitive cells (Fig. 3B). In addition, exposure to capsaicin excited a larger cohort of neurons (55%), encompassing all of the formalin-sensitive cells, consistent with the expression profile of TRPA1 channels (Fig. 3A and B) (16, 17, 20). These responses were significantly attenuated by ruthenium red (data not shown). Neurons from *TRPA1*<sup>-/-</sup> mice were completely unresponsive to formalin or AITC (Fig. 3C) but retained normal sensitivity to capsaicin [Fig. 3A and B (20)]. At higher concentrations of formalin ( $>0.025\%$ ), all neurons showed a small slowly developing increase in intracellular calcium, presumably reflecting nonspecific and irreversible cellular toxicity.

Cultured rat DRG neurons also showed increases in intracellular calcium concentration in response to 0.01% formalin. All cells that responded to formalin also responded to AITC. These responses were blocked by HC-030031 (data not shown). Together, these

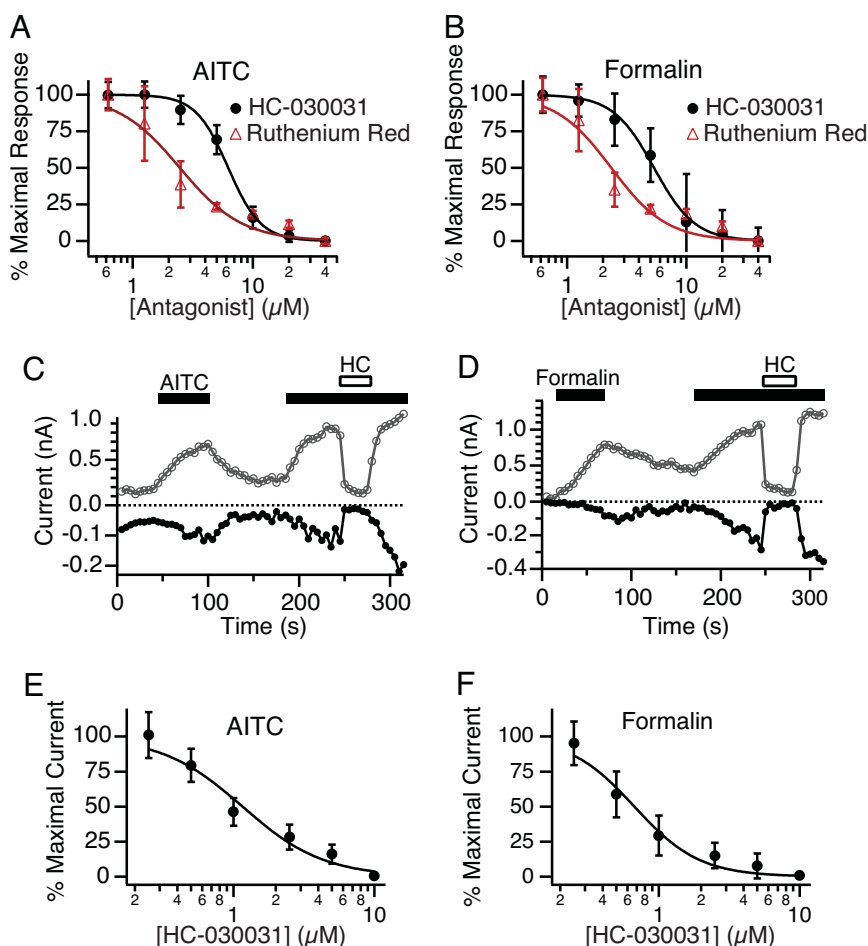


**Fig. 2.** Block of TRPA1 by ruthenium red and HC-030031. (A and B) Concentration-dependent inhibition of calcium responses by HC-030031 (black) or ruthenium red (red) in hTRPA1 cells activated by AITC (A) or formalin (B). Each point represents the average response of 18 experiments,  $\approx 3$  min after stimulation. (C and D) Time course of inward (closed circles) and outward (open circles) currents recorded in the perforated patch configuration for single representative cells activated by AITC (5  $\mu$ M; C) or formalin (0.01%; D) and blocked by addition of HC-030031 (10  $\mu$ M, HC, open bar). (E and F) Concentration-dependent inhibition of AITC- (E) or formalin- (F) evoked currents by HC-030031 in hTRPA1 expressing cells. Each point represents the average of five independent cells; values represent mean  $\pm$  SEM.

results demonstrate that TRPA1 is the sole target for the specific excitatory actions of formalin on sensory neurons.

**Pharmacologic or Genetic Disruption of TRPA1 Blocks Formalin-Evoked Pain.** To assess the role of TRPA1 in the *in vivo* response to formalin, we first investigated the effects of HC-030031 on formalin-evoked pain behaviors in rats using an automated flinch-detecting system (10). Intraperitoneal administration of HC-030031 preceding formalin injection decreased the number of flinches observed in Phase I in a dose-dependent fashion (Fig.

4A and B). At the highest concentration of HC-030031, flinching was reduced to levels similar to those observed with saline injection. HC-030031 also decreased the number of flinches in Phase II, primarily affecting responses within the early component (Phase IIA) of this segment (Fig. 4A). In contrast, gabapentin, which is widely used to treat neuropathic pain, had no significant effect on Phase I but significantly reduced the number of flinches observed in Phase II, as reported (11, 12, 25), with the major effect seen in Phase IIB (Fig. 4A and B).

The effects of HC-030031 and gabapentin were also tested in an AITC-induced flinching model. After injection of AITC (50  $\mu$ l of 10%) into the rat hind paw, HC-030031 (300 mg/kg) significantly reduced flinching during the first 5 min, whereas the same dose of gabapentin had no significant effect (Fig. 4C). Over the remainder of the hour, both gabapentin and HC-030031 decreased flinch frequency, a result that mirrors the effects observed on formalin-induced flinching (Fig. 4B). Impaired locomotor function did not account for the reduced flinching, because HC-030031 (at dose levels  $\leq 300$  mg/kg *i.p.*) had no effect in an accelerating rotarod test. In contrast, gabapentin significantly decreased performance in this test, consistent with previous results (12) (Fig. 4D).

To corroborate a role for TRPA1 in mediating formalin-induced flinching, we examined formalin-evoked behavior in

**Table 1. Analysis of HC-030031 specificity**

Channel	Activator	IC <sub>50</sub> , $\mu$ M
hTRPA1	AITC	0.7 $\pm$ 0.1
hTRPA1	Formalin	1.2 $\pm$ 0.2
hTRPV1	Capsaicin	>20
hTRPV3	2-APB	>10
hTRPV4	4 $\alpha$ -PDD	>10
hERG	Voltage	>20
NaV 1.2	Voltage	>20

2-APB, 2-aminoethyl diphenylborinate; 4 $\alpha$ -PDD, 4 $\alpha$ -phorbol 12,13-didecanoate.

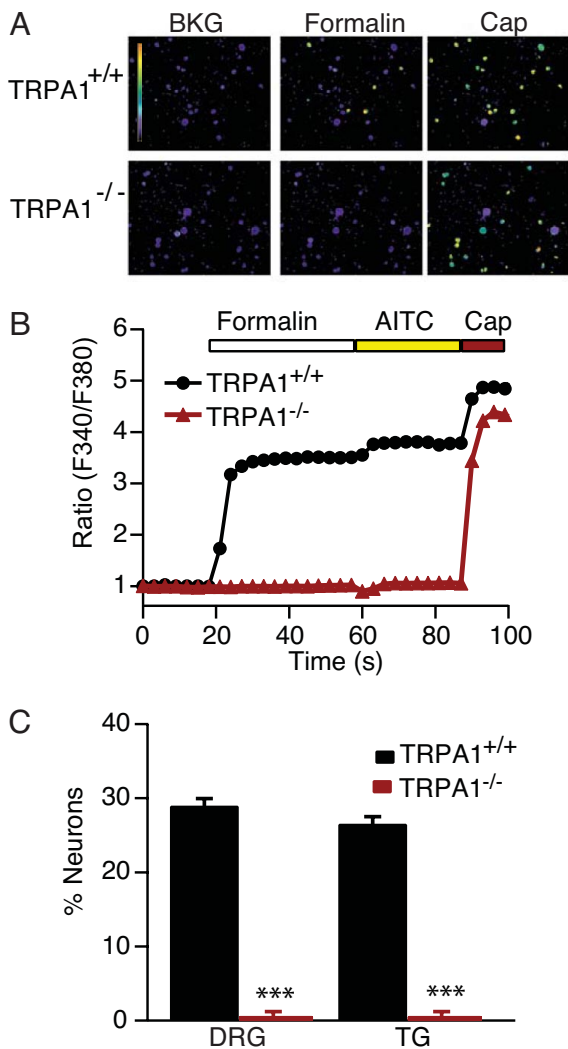


**Fig. 3.** DRG neurons from TRPA1-deficient mice are unresponsive to formalin. (A) Pseudocolor ratiometric images of DRG neurons acutely isolated from TRPA1<sup>+/+</sup> and TRPA1<sup>-/-</sup> mice loaded with the calcium indicator Fura-2. Formalin application elicited a calcium response in TRPA1<sup>+/+</sup> neurons. No formalin sensitivity was detected in neurons from TRPA1-deficient mice, whereas capsaicin sensitivity was unperturbed. (B) Representative responses of DRG neurons to formalin, AITC, and capsaicin. Traces represent an average of 15 cells cultured from TRPA1<sup>+/+</sup> (black) or TRPA1<sup>-/-</sup> (red) mice. (C) Quantification of responses to formalin in neurons isolated from TRPA1<sup>+/+</sup> (black) or TRPA1<sup>-/-</sup> (red) mice ( $n \geq 328$  per genotype; \*,  $P < 0.05$ ; \*\*,  $P < 0.01$ ; \*\*\*,  $P < 0.001$ ; Student's *t* test).

mice lacking functional TRPA1 channels (20). Sensory neurons from TRPA1-deficient mice do not respond to AITC or acrolein. Moreover, these animals do not exhibit acute behavioral responses or the thermal or mechanical hypersensitivity normally associated with topical application of AITC (20, 21). We found that these animals also displayed significantly attenuated responses in Phase I of the formalin test when compared with WT littermates (Fig. 5). The Phase II response was also significantly diminished. Interestingly, this decrease in licking and lifting behaviors was seen in both Phase IIA and IIB.

The results presented here support the hypothesis that formalin elicits pain-related behaviors by activating TRPA1 on primary afferent nociceptors. Additionally, these findings suggest that HC-030031 blocks formalin-evoked responses *in vivo* through its inhibitory actions on TRPA1.

## Discussion

We have shown that TRPA1 is required for the generation of formalin-induced pain behaviors in rodents. Formalin also activates TRPA1 in a heterologous expression system. At formalin concentrations of 0.01%, representing a 250-fold dilution from the concentration injected *in vivo*, this activation appears to be mediated solely by TRPA1. All AITC-sensitive mouse DRG neurons responded to formalin, and neither AITC nor formalin activated a calcium response in neurons from TRPA1<sup>-/-</sup> animals. In addition, the selective TRPA1 antagonist HC-030031 blocked both AITC- and formalin-induced currents and calcium responses with similar IC<sub>50</sub> values. Taken together, these results support the conclusion that TRPA1 is the principal site of formalin action.

The selective antagonist, HC-030031, provides a useful pharmacological tool to study the role of TRPA1. HC-030031 reversibly blocks TRPA1 currents with a similar potency, regardless of the agonist used; this includes blockade of currents elicited by reversible agonists, such as AITC, or irreversible agonists, such as *N*-methyl maleimide. Formalin-induced currents, which appear partially reversible, are also efficiently blocked. These data suggest that the inhibition is unlikely to be competitive, although at present the mechanism of block for this small molecule antagonist is uncertain. TRPA1 inhibition by HC-030031 nearly eliminated pain-related flinching in both phases of the formalin response *in vivo* and also greatly attenuated AITC-induced flinching. The efficacy of HC-030031 in these models parallels the results observed in TRPA1<sup>-/-</sup> mice, where formalin-evoked pain is significantly reduced. There does remain a small but finite residual response at all phases of the assay, but the nature of this component and whether it derives from a direct action of formalin on the primary afferent nerve fiber remain to be determined.

Our results reveal the molecular mechanism of formalin-induced pain. Formaldehyde, the active ingredient in formalin, is a fixative that covalently cross-links proteins in a nonspecific fashion. This cross-linking leads to a variety of effects, including general tissue damage. We show that, rather than inducing neuronal activity in response to nonspecific tissue damage, formalin specifically activates TRPA1 and drives the firing of a subpopulation of C fibers. The mechanism of this activation likely parallels that of other TRPA1 agonists, which induce covalent modification of cysteine and lysine residues (22, 23). In this way, formalin-evoked TRPA1 activation drives the CNS sensitization that underlies Phase II of the formalin response (5, 6, 13). Other formalin-based models, such as those for temporomandibular jaw disorder and facial pain, are also likely to be TRPA1-dependent. On a longer timescale, formalin produces blistering and edema, which peak between 4 and 5 h after injection, significantly later than the peak of pain behaviors traditionally measured in animal models (13). Understanding the relative contribution of afferent-induced neurogenic inflammation and direct local cellular injury due to nonspecific effects of formaldehyde will require further investigation.

Recognition of the key role of TRPA1 in formalin-induced pain resolves the longstanding uncertainty surrounding the mechanism of this widely used model. Our results, combined with recent reports of pain deficits in TRPA1<sup>-/-</sup> mice (20, 21), suggest that TRPA1 is a useful target for the development of novel analgesics.

## Materials and Methods

**Cells.** Full-length hTRPA1, TRPV1, TRPV3, TRPV4, and rTRPA1 cDNAs were subcloned into pCDNA5/TO (Invitrogen, Carlsbad, CA). Stable clonal 293-T-Rex cell lines (Invitrogen) were selected in 100  $\mu$ g/ml hygromycin and grown according to the manufacturer's instructions.

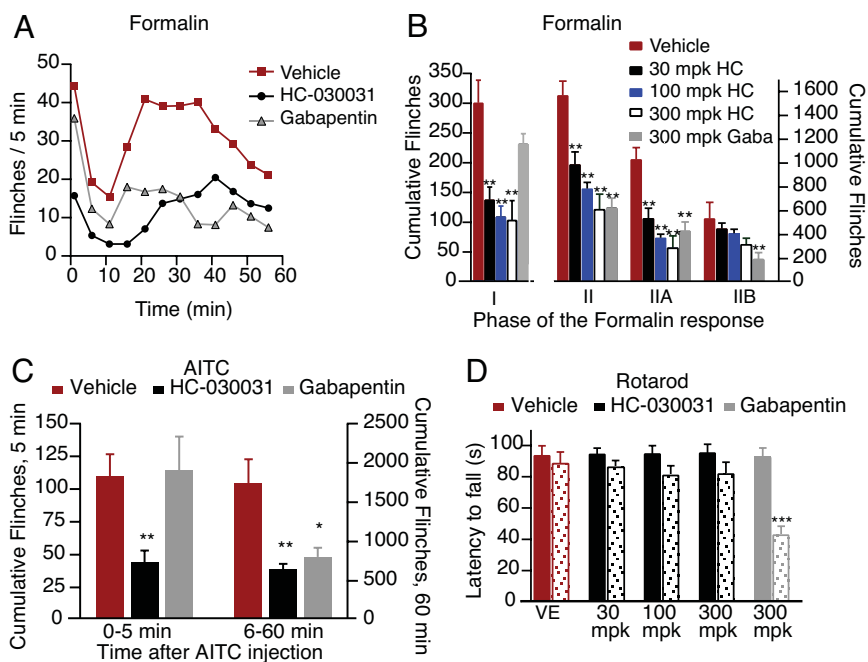


**Fig. 4.** HC-030031 inhibition of TRPA1 attenuates formalin- and AITC-evoked pain behavior. (A) Time course of flinching in animals treated with formalin, as measured using an automated flinch-detection system. Animals pretreated with a single injection of gabapentin (300 mg/kg i.p.; gray triangles;  $n = 8$ ) or HC-030031 (black circles;  $n = 7$ ) showed significantly less flinching compared with vehicle-treated animals (red squares;  $n = 7$ ). (B) Quantification of the formalin response binned into different phases. Animals were pretreated with vehicle (red,  $n = 7$ ), HC-030031 at 30 mg/kg (black,  $n = 7$ ), 100 mg/kg HC-030031 (blue,  $n = 8$ ), 300 mg/kg HC-030031 (white,  $n = 7$ ), or 300 mg/kg gabapentin (gray,  $n = 8$ ). Phase I (0–9 min), Phase II (10–60 min), Phase IIA (10–40 min), and Phase IIB (41–60 min). (C) Animals injected with the TRPA1 agonist, AITC, showed significant flinching that was unaffected by pretreatment with vehicle (red). In contrast, pretreatment with 300 mg/kg of the TRPA1 antagonist, HC-030031 (black), greatly reduced the flinching observed during the initial 5 min of the response to AITC. Pretreatment with gabapentin (gray) had no effect during this initial phase. During the second phase of the response (6–60 min), both HC-030031 (black) and gabapentin (gray) had an analgesic effect. (D) HC-030031 (black) has no effect on rotarod performance ( $n = 8$ ). Latencies to fall were measured immediately before (solid) and 1 h after (stippled) compound treatment. No significant effect was seen with HC-030031 at dose levels  $\leq 300$  mg/kg i.p. Gabapentin (300 mg/kg i.p., gray) significantly decreased time spent on the rotarod compared with uninjected or vehicle-injected controls (red). \*,  $P < 0.05$ ; \*\*,  $P < 0.01$ ; \*\*\*,  $P < 0.001$ ; one-way ANOVA, followed by a Bonferroni multicomparison test.

**Ca<sup>2+</sup> Measurements of Recombinant Cell Lines.** Cells were plated in 384-well plates. Cells were loaded with 1  $\mu$ M Fluo-4 and 0.05% pluronic acid for 1 h at room temperature. Formalin-selectivity experiments were run with 0.003% formalin. Agonist EC<sub>50</sub> curves used 0–25  $\mu$ M AITC or 0–0.017% formalin. IC<sub>50</sub> curves for TRPA1 antagonists were constructed by using 0.625–40  $\mu$ M antagonist in the presence of 5  $\mu$ M AITC or 0.001% formalin using data collected 3 min after agonist addition. Data were collected by using a Hamamatsu (Hamamatsu City, Japan)

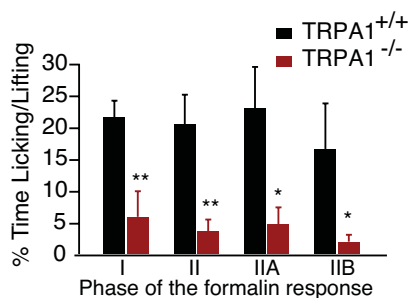


**Fig. 5.** TRPA1-deficient mice display significantly reduced formalin-evoked pain behavior. Time spent licking and lifting was assessed manually in TRPA1<sup>+/+</sup> (black) and TRPA1<sup>-/-</sup> (red) littermates. Licking and lifting were substantially attenuated in TRPA1-deficient animals during all phases of the formalin test when compared with WT littermates ( $n = 7$  per genotype; \*,  $P < 0.05$ ; \*\*,  $P < 0.01$ ; \*\*\*,  $P < 0.001$ ; Student's *t* test).

FDSS 6000 fluorescence-based plate reader and analyzed using IGOR Pro.

**Electrophysiology.** For TRPA1 recordings, Ca<sup>2+</sup>-free external solution was used, consisting of 145 mM NaCl, 10 mM Hepes, 10 mM glucose, 4.5 mM KCl, 1 mM EGTA, 3 mM MgCl<sub>2</sub>, and pH to 7.4, with NaOH. For other channels, normal Ringer was used, with the identical formulation except lacking EGTA and with 2 mM CaCl<sub>2</sub> and 1 mM MgCl<sub>2</sub>. Cesium aspartate (CsAsp) internal solution consisted of 140 mM CsAsp, 10 mM EGTA, 10 mM Hepes, 2.27 mM MgCl<sub>2</sub>, and 1.91 mM CaCl<sub>2</sub>, pH to 7.2, with CsOH, with a calculated free Ca<sup>2+</sup> of 50 nM (MaxChelator; Chris Patton, Stanford University, Palo Alto, CA). For perforated patch recordings, freshly prepared amphotericin was added to this solution at 0.6 mg/ml. Recordings were made by using an Axon Multiclamp 700B amplifier (Molecular Devices, Sunnyvale, CA) and pClamp 9.0 (Molecular Devices) software. Data were filtered at 4 kHz. For all experiments, the holding potential was  $-40$  mV. Cells were ramped every 5 s from  $-120$  to  $+100$  mV over the course of 400 ms. Inward and outward currents were analyzed from the ramps at  $-80$  and  $+80$  mV, respectively. Solutions were switched by using a gravity-fed continuous focal perfusion system.

**Chemicals.** A 10% low-odor formalin solution containing 4% wt/vol formaldehyde, 0.075 M sodium phosphate, 1.5% wt/vol methanol, and phosphate buffer was used for all experiments (Formalde-Fresh; Fisher Scientific, Waltham, MA). AITC so-

lution was prepared fresh daily (Sigma–Aldrich, St. Louis, MO). HC-030031 was obtained from ChemBridge (San Diego, CA).

**DRG and Trigeminal Calcium Imaging.** DRG and trigeminal neurons were isolated and calcium imaging experiments were performed as described by using Fura-2 as the indicator (17, 20).

**Animals.** All experiments involving animals were performed in accordance with Institutional Animal Care and Use Committee procedures and protocols. For the formalin test in rats, we used an automated flinch-detecting system (T. Yaksh, University of California at San Diego, La Jolla, CA) (10). On the day of testing, a small metal band (0.5 g) was loosely placed around the right hind paw of a male Sprague–Dawley rat (average weight,  $\approx$ 250 g). Rats were allowed to acclimate to a Plexiglas chamber for at least 30 min before testing. Formalin was then injected (50  $\mu$ l of 2.5% formalin, diluted in saline) into the dorsal surface of the right hind paw of the rat, and the animal was put into a chamber of the automated formalin apparatus where movement of the formalin-injected paw was recorded. The number of paw flinches was tallied by minute over the next 60 min. Phases were defined as follows: Phase I (0–9 min), Phase II (10–60 min), Phase IIA (10–40 min), and Phase IIB (41–60 min). Upon completion of the test, animals were removed and killed. AITC-induced flinching experiments were carried out identically, with

the exception that animals were injected with 10% AITC instead of formalin. For the mouse formalin tests, animals were allowed to habituate to Plexiglas chambers for at least 5 min; 10  $\mu$ l of a 0.5% formalin solution was injected into one of the hind paws, and flinches as well as time spent licking were recorded by a blinded observer.

Locomotor function, coordination, and sedation of animals were tested by using a rotarod apparatus, as described (12) (Accuscan Instruments, Columbus, OH). The rotarod was programmed to accelerate to 20 rpm in 120 sec. All rats were trained 1 day before the study. On the second day, each rat underwent two trials before the treatment to determine the baseline. Effects of compounds were assessed 60 min after a single i.p. injection. The latency of falling from the rotarod was recorded for each animal. Cutoff time was 120 sec.

We thank Jennifer Gaines for cell culture support and Jeannie Poblete for mouse husbandry and genotyping. We are also grateful to Colby Cook for help with the rotarod assay. We thank Drs. David Clapham, Glenn Larsen, Clifford Woolf, Roger Nicoll, Cheryl Stucky, and Howard Fields for helpful suggestions on the manuscript. This work was supported in part by grants from the National Institutes of Health (D.J.), a Burroughs Wellcome Fund Career Award in Biomedical Sciences (D.M.B.), and a postdoctoral fellowship from the International Human Frontier Science Program Organization (J.S.). We also thank Tony Yaksh, Damon McCumber, and the University of California at San Diego for pilot experiments and for the automated flinching apparatus.

1. Dubuisson D, Dennis SG (1977) *Pain* 4:161–174.
2. Abbott FV, Franklin KB, Westbrook RF (1995) *Pain* 60:91–102.
3. Tjolsen A, Berge OG, Hunskaar S, Rosland JH, Hole K (1992) *Pain* 51:5–17.
4. Abbadie C, Taylor BK, Peterson MA, Basbaum AI (1997) *Pain* 69:101–110.
5. Coderre TJ, Vaccarino AL, Melzack R (1990) *Brain Res* 535:155–158.
6. Woolf CJ (1983) *Nature* 306:686–688.
7. Malmberg AB, Yaksh TL (1992) *J Pharmacol Exp Ther* 263:136–146.
8. Yoon MH, Bae HB, Choi JI, Jeong SW, Chung SS, Yoo KY, Jeong CY, Kim SJ, Chung ST, Kim CM, An TH (2005) *Pharmacology* 75:157–164.
9. Coderre TJ, Melzack R (1992) *J Neurosci* 12:3671–3675.
10. Yaksh TL, Ozaki G, McCumber D, Rathbun M, Svensson C, Malkmus S, Yaksh MC (2001) *J Appl Physiol* 90:2386–2402.
11. Singh L, Field MJ, Ferris P, Hunter JC, Oles RJ, Williams RG, Woodruff GN (1996) *Psychopharmacology (Berl)* 127:1–9.
12. Field MJ, Oles RJ, Lewis AS, McCleary S, Hughes J, Singh L (1997) *Br J Pharmacol* 121:1513–1522.
13. Dickenson AH, Sullivan AF (1987) *Pain* 30:349–360.
14. Story GM, Peier AM, Reeve AJ, Eid SR, Mosbacher J, Hricik TR, Earley TJ, Hergarden AC, Andersson DA, Hwang SW, et al. (2003) *Cell* 112:819–829.
15. Nagata K, Duggan A, Kumar G, Garcia-Anoveros J (2005) *J Neurosci* 25:4052–4061.
16. Kobayashi K, Fukuoka T, Obata K, Yamanaka H, Dai Y, Tokunaga A, Noguchi K (2005) *J Comp Neurol* 493:596–606.
17. Jordt SE, Bautista DM, Chuang HH, McKemy DD, Zygmunt PM, Hogestatt ED, Meng ID, Julius D (2004) *Nature* 427:260–265.
18. Macpherson LJ, Geierstanger BH, Viswanath V, Bandell M, Eid SR, Hwang S, Patapoutian A (2005) *Curr Biol* 15:929–934.
19. Bautista DM, Movahed P, Hinman A, Axelsson HE, Sterner O, Hogestatt ED, Julius D, Jordt SE, Zygmunt PM (2005) *Proc Natl Acad Sci USA* 102:12248–12252.
20. Bautista DM, Jordt SE, Nikai T, Tsuruda PR, Read AJ, Poblete J, Yamoah EN, Basbaum AI, Julius D (2006) *Cell* 124:1269–1282.
21. Kwan KY, Allchorne AJ, Vollrath MA, Christensen AP, Zhang DS, Woolf CJ, Corey DP (2006) *Neuron* 50:277–289.
22. Hinman A, Chuang HH, Bautista DM, Julius D (2006) *Proc Natl Acad Sci USA* 103:19564–19568.
23. Macpherson LJ, Dubin AE, Evans MJ, Marr F, Schultz PG, Cravatt BF, Patapoutian A (2007) *Nature* 445:541–545.
24. Xu H, Blair NT, Clapham DE (2005) *J Neurosci* 25:8924–8937.
25. Urban MO, Ren K, Park KT, Campbell B, Anker N, Stearns B, Aiyar J, Belley M, Cohen C, Bristow L (2005) *J Pharmacol Exp Ther* 313:1209–1216.